SUPPORTING INFORMATION

Guiné V.[1], Spadini L.[2], Muris M.[3], Sarret G.[2], Delolme C.[3], Gaudet J-P.[1], and Martins J.M.F.[1*]

Zinc sorption to cell wall components of three gram-negative bacteria: a combined titration, modeling and EXAFS study.

[1] Laboratoire d'étude des Transferts en Hydrologie et Environnement (LTHE), Domaine Universitaire, BP53, 38041 Grenoble Cedex 9, France.

[2] Environmental Geochemistry Group, LGIT, University J. Fourier and CNRS, BP 53, 38041 Grenoble Cedex 9, France.

[3] Laboratoire des Sciences de l'Environnement (LSE) - E.N.T.P.E. - Rue Maurice Audin - 69518 Vaulx-en-Velin Cedex - France.

[*]corresponding author: jean.martins@hmg.inpg.fr

The supporting information section contains 12 text pages including 3 figures.

Material and Methods

Cells enumeration

Cell concentrations were determined using the following fast indirect methods: *E. coli* and *C. metallidurans* cell concentrations were obtained from the absorbance at 600 nm (A_{600}) on a Perkin Elmer UV/VIS spectrometer. Because *P. putida* suspensions were not turbid enough, enumeration was based on protein quantification (Lowry's method). A_{600} and protein content were related to colony forming units (CFU) by agar plate counts. The relation between CFU and bacterial mass (g_{DW}, DW: dry weight) was obtained from five replicated filtrations (0.2µm), dryings (24h/105°C) and weightings (Table 1).

Bacterial electrophoretic mobility (Zeta potential)

Electrophoretic mobility measurements were performed in triplicate for the three strains in the pH range 2.5 to 9.0 (10 mM sodium salt solutions) with a ZetaSizer 3000HS (Malvern Instruments). The electrophoretic mobility of bacterial cells is expressed as a potential (mV) given by the calibrated Zetameter device. These measurements permitted the determination of the isoelectric point (pH_{IEP} mV), *i.e.* the pH of assumed null electrophoretic mobility and consequently null particle charge. At this pH the surface charge and electrical double layer are both neutralized within the limits of experimental significance. Consequently, $pH_{IEP} \cong pH_{PZNPC}$ (Point of Zero Net [no metals] Proton surface Charge). The graphically determined pH_{PZNPC} situates around pH 3.5 (Fig. S1, Table 1) for the three strains, evidencing that the bacterial colloids are negatively charged in the acid-base titration pH range (pH 4 to 10). This attests for the predominance of negatively charged groups (carboxyl and phosphodiester) over positively charged groups (amine) in the environmental pH range. Conceptually, at the pH_{PZNPC} the positive

charge of amines counterbalances the negative charges of strongly acidic carboxyl groups (*e.g.* amino acids, which present pK values ≈ 2). Beyond the point of zero charge, the zeta potential may not be easily correlated to surface charge as other parameters such as electrolytic conductance properties interfere (*1*).

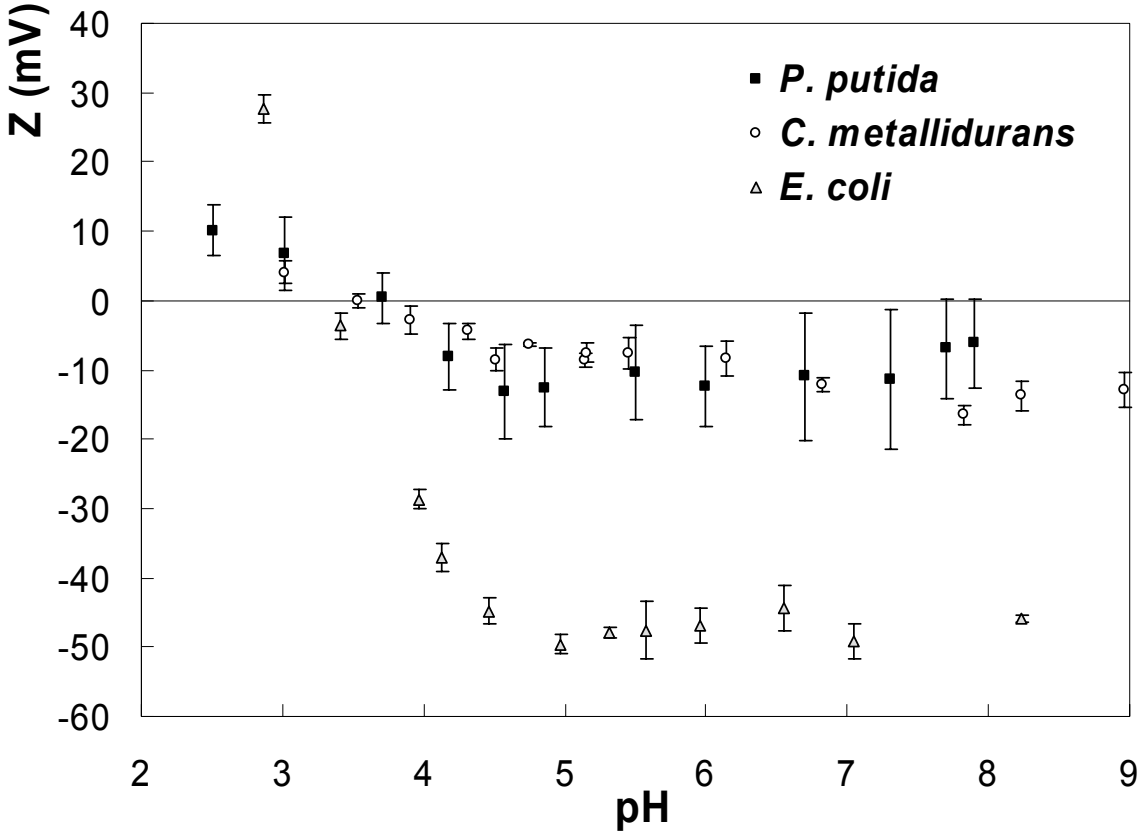

Figure S1: Electrophoretic mobility of *C. metallidurans*, *E. coli* and *P. putida* cells at different pH measured with a Zetasizer 3000 HS (Malvern).

Acid-base titration experiments

Acid-base titrations were performed in a closed vessel under N_2 positive pressure. 50 ml of bacterial suspensions of 2±0.4 g_{DW} L^{-1} were stirred and maintained at 4°C (*E. coli* and *C.*

metallidurans) or 20°C (*P. putida*). In the case of *E. coli* and *C. metallidurans* at 20°C the potential of the pH electrode did not stabilized within a reasonable timescale whereas at 4°C reproducible measurements were obtained. Titrations were performed from equilibrium pH of the cell suspensions (pH 5 to 7) towards pH 4 or 10 adding strong acid or base stepwise, respectively. This procedure avoids irreversible effects on bacteria such as cell aggregation and membrane denaturizing. The data treatment was based on the proton mass balance:

$$[H^+] = \frac{v_0[H_I]}{v_0 + v} + \frac{v[H_B]}{v_0 + v} + \frac{v_0[H_S]}{v_0 + v} + [OH^-]$$

where: $[H^+]$ the free proton concentration; $[H_I]$ the analytically known initial concentration of strong acid (positive) or base (negative) added to the reactor; $[H_B]$ the buret strong acid (positive) or base (negative) concentration; $[H_S]$ the experimentally assessed concentration of protons released from the weak ligand (*i.e.* the bacterial substrate); $[OH^-]$ the protons generated from water dissociation:

$K_W^{0,01}(25°C) = [OH^-][H^+] = 10^{-13.91}$; v_0 the initial reactor volume and v the buret volume added to reactor.

$[H^+] = 10^{(E-E°)/k}$ was calibrated to the electrode potential E (mV) by titrating before each experiment known concentration standards in the background electrolyte. $E°$ and k (mV) refer to the concentration based Nernst parameters. In electrode calibration $[H_S]$ should be zero and thus represents the residual of the calibration (R). R increases exponentially at low and high pH. Confronting bacterial $[H_S]$ to calibration R data revealed the pH domain (pH<4 and pH>10) where $[H_S]$ data are non significant with respect to the uncertainty in $[H^+]$. Then these data were omitted.

Titration reversibility was studied in duplicate with *P. putida* (data not shown) assuming a similar behavior of the other two bacteria. After completion of each half-titration a second titration was performed in the opposite pH direction by adding strong acid or base depending on

the end pH of the first titration (4 or 10). These experiments resulted in a good agreement between up and down titrations (less than 5% difference) indicating a complete reversibility of proton exchange.

Cell viability was tested after each titration experiments and indicated (about 70% survivals) that the soft acid and base treatments did not damage the bacteria.

Acid-base titration modeling

In modeling three acid-base exchange sites were discriminated within the investigated pH range following Fein *et al.* (*2*), noted:

(1) Acidic site: $\equiv COOH \leftrightarrow \equiv COO^- + H^+$; $2 \leq pK_{x\text{-}CH} \leq 6$; $[T_{x\text{-}CH}]$;

(2) Neutral site: $\equiv POH \leftrightarrow \equiv PO^- + H^+$; $5.7 \leq pK_{x\text{-}PH} \leq 7.2$; $[T_{x\text{-}PH}]$;

(3) Basic site: $\equiv NH^+ \leftrightarrow \equiv N + H^+$; $8 \leq pK_{x\text{-}NH} \leq 12$; $[T_{x\text{-}NH}]$.

They are respectively representative for carboxyl and phosphodiester (1), phosphomonoester (2) and hydroxyl and amine (3) functional groups. x = CM for *C. metallidurans*, EC for *E. coli* and PP for *P. putida*. $[T_{x\text{-}CH}]$, $[T_{x\text{-}PH}]$ and $[T_{x\text{-}NH}]$ refer to the total concentrations of these respective sites. The sum of the three terms expresses the model based total proton exchange capacity of one bacterial strain.

At titration start-point $[H_S] \cong [H^+]$, $[H_S]$ is normalized to the titration initial pH, which is essentially controlled by not assessable proton sources, e.g. the pH buffering growth media. Modeling requires $[H_S]$ to be normalized to a quantifiable reference mass balance state (*3-5*):

$$[H_{S\text{-}Ref}] = [H_S] + [H_0] = [\equiv COO^-] + [\equiv PO^-] + [\equiv N]$$

This expresses the proton concentration released to solution from the fully protonated model ligand (the proton mass balance reference state chosen in this study), and $[H_0]$ conceptually

represents the proton concentration released from the model ligand to the solution at the titration start pH.

The measured and modeled pH_{PZNPC}, determined from the electrophoretic mobility measurements (Fig. S1) cannot be compared as the basic model site (noted $\equiv NH^{+}$) involves amine and hydroxyl functional groups, i.e. differently charged contributions in unknown proportions. Thus $[H_0]$ cannot be analytically determined and was consequently obtained by scaling model $[H_{S\text{-}Ref}]$ to experimental $[H_S]$ data. That means adding for one titration data series a constant offset to each $[H_{S\text{-}Ref}]$ model data point (data in dilution corrected units, e.g. mol g_{DW}^{-1}). It has to be noted that the presented equilibrium model involves only a subset of all acid-base sites: strongly acidic and basic sites are not considered as they situate outside the experimentally assessable pH range of the titrations.

Equilibrium analysis based on a non-electrostatic model was performed with GRFIT (*6*). This FITEQL substitute permits visual comparison of fitted and experimental data. For example, graphical fitting of metal sorption data is possible by adjusting both numerically or manually the equilibrium variables. As outlined in the discussion section, the reactivity situates in the exopolysaccharides (EPS) and/or in the inner cell space. As EPS structure is difficult to characterize, the modelling approach to be applied: 'flat plane models' such as the constant capacitance model, Donnan-type models for gel forming macromolecules or a non-electrostatic model considering highly dispersed charges, is unclear. Fein *et al.* (*5*) demonstrated that acid-base titrations of *Bacillus subtilis* did not allow discriminating surface electrostatic effects. We consider that the introduction of physically unconstrained models will not help elucidating the processes and variables which control metal sorption on bacteria. Thus the equilibrium analysis was based on a non-electrostatic model.

EXAFS data extraction and analysis

Zn K-edge EXAFS data extraction was done according to standard methods. The k^3-weighted EXAFS spectra for the Zn-sorbed bacteria were least-squares simulated by a combination of two to three Zn reference compounds over a wave vector (k) range of 2.0 - 11.5 $Å^{-1}$ from a library of mineral and organic Zn compounds. The best simulations, defined as the simulations whose normalized sum-squares residual (*NSS*) was comprised between the value obtained for the best simulation (NSS_{best}) and 1.1 NSS_{best}, were used to calculate the mean and standard deviation for each Zn species. For the first shell simulation, EXAFS spectra were Fourier transformed over a k range of 3.5 - 11.5 $Å^{-1}$, and the contribution of the first coordination shell ($R + \Delta R$ range : 1.1 - 2.3 Å) was back-transformed and simulated in k and R space. Theoretical standards based on the known structures of sphalerite (*7*) for the Zn-S pair and of Zn malate (*8*) for the Zn-O pair were generated by FEFF7 (*9*). Energy shifts were constrained at the values found for Zn malate and ZnS references (5 and 6 eV, respectively) ± 2 eV. The preparation of Zn-sorbed hydroxylapatite is described in Panfili *et al.* (*10*), and of Zn malate is described in Sarret *et al.* (*11*). The spectrum for Zn-cysteine standard at a ligand/metal ratio (L/M) of 10 was provided by S. Beauchemin (*12*), and the Zn cysteine at L/M=5 was prepared by precipitation of 10 mM Zn nitrate with 50 mM L-cysteine. EXAFS spectra were treated by linear combination fits (LCFs) using a library of Zn references (Fig. 4, Fig. S2 and Table 2). This library includes (i) simple compounds in which Zn is bound to carboxyls (Zn acetate anhydrous and dihydrate, Zn oxalate dihydrate, Zn malonate, Zn benzoate anhydrous, Zn formate hydrate, and Zn succinate in solution), to carboxyls and hydroxyls (Zn citrate dihydrate and in solution and Zn malate), to carboxyls and amines (Zn histidine, Zn aspartate, and Zn glycine, all in solution), to sulfhydryls (Zn cysteine at L/M=10, precipitated), and to sulfhydryls and carboxyls groups (Zn cysteine at L/M=5, precipitated), and (ii) complex structures such as freeze-dried Zn-humic acid complexes at various Zn concentrations.

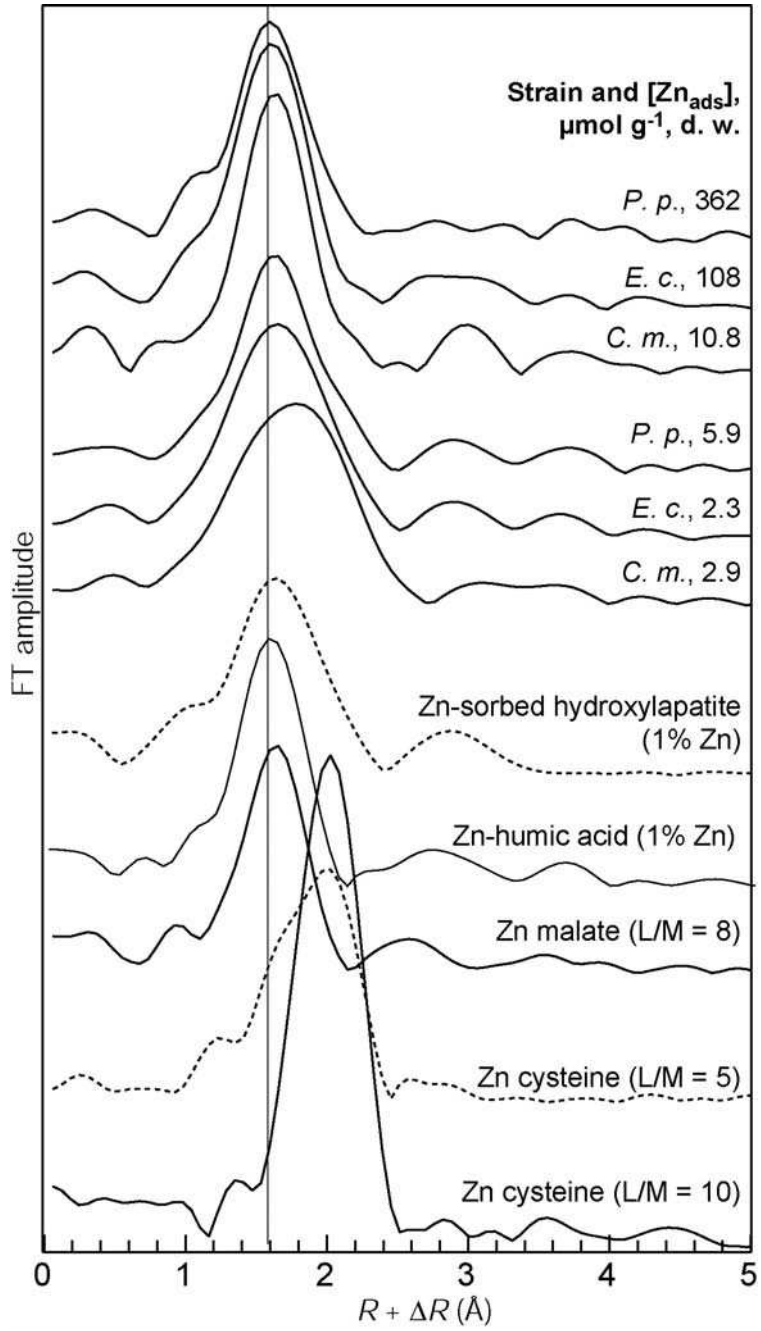

Figure S2: Fourier transforms of spectra EXAFS of the Zn-sorbed bacteria and Zn reference compounds.

The spectrum shown in Figure 4 is a Zn-humic acid (IHSS 1S102H) containing 1% Zn, prepared as follows: 0.5 g of HA was introduced in ultrapure water. The pH was increased to 12 with

NaOH 1M to dissolve the HA, and then decreased to 6.0 using HNO_3 0.5 M. 7.6 ml of 10^{-2} M $Zn(NO_3)_2$ were introduced at a rate of 1 ml/min, the pH being maintained at 6.0 with NaOH 0.1 M during 24h. The solution was then dialyzed with a Spectra-Por 6 membrane to remove excess Zn, and the solution was finally freeze-dried. The P-containing references include Zn-phosphate minerals (hopeite, parahopeite, Zn phosphate dihydrate, and phosphophyllite), Zn-sorbed hydroxylapatite at various Zn loadings and pH (1% Zn and pH 6.0 for the spectrum shown in Figure 4) as proxies for Zn bound to a distribution of phosphate surface sites (*9*), and Zn phytate. Phytic acid $(CH)_6(OPO_3H_2)_6$ is a cyclic molecule containing six phosphomonoester groups, and Zn binds to one or several phosphomonoester groups. Our library contains no reference for Zn bound to phosphodiester groups.

EXAFS results

For the two bacterial samples in which Zn is bound to O and S neighbors (*C. metallidurans* and *E. coli* at low Zn loading), the number of S atoms bound to Zn was calculated by multiplying S coordination number (2.5 and 1.5, respectively) by the total Zn content (2.9 and 2.3 µmol g_{DW}^{-1}, respectively; this calculation assumes that there is no S atom in a bridging position between two Zn atoms). This leads to 7.25 and 3.45 µmol of S atoms bound to Zn per g_{DW} in *C. metallidurans* and in *E. coli* at low Zn loadings, respectively. Considering that both bacteria contain 0.54 wt.% sulfur (See Materials and Methods section), these quantities represent 4.3 and 2.1 % of the total S content, respectively.

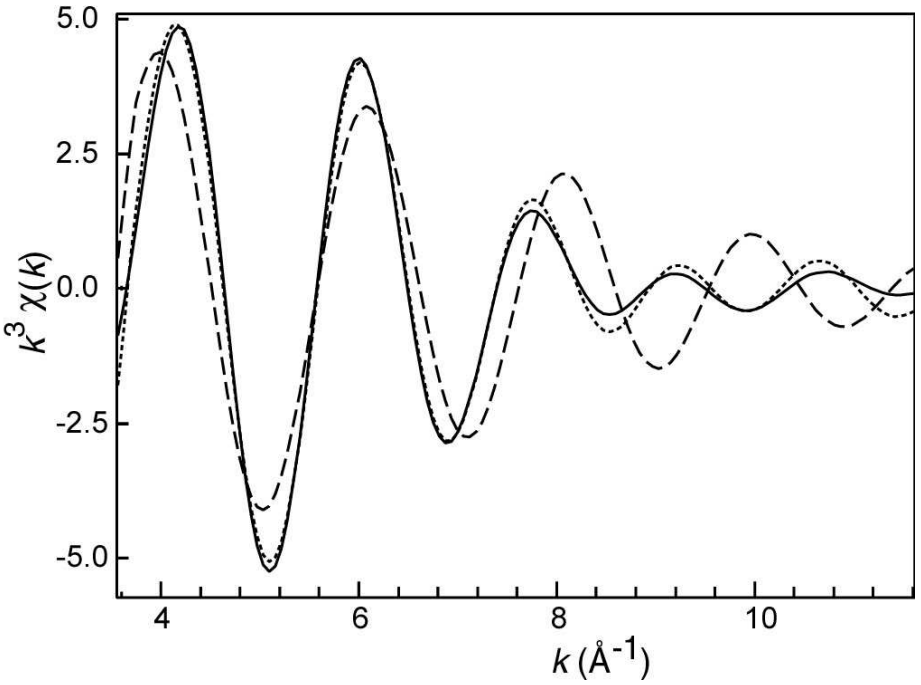

Figure S3: Best fits obtained for the first shell of *C. metallidurans* CH34 containing 2.9 µmol Zn g_{DW}^{-1} (plain line) using a single O shell (dashed line, d(Zn-O) = 2.07 Å) and one O and one S shell (dotted lines, distances given in Table 2). Clearly, this contribution cannot be simulated by oxygen atoms only.

References

(1) Khilar K. C. and Fogler H. S. (1987) "Colloidally induced fines migration in porous media", *Rev. Chem. Eng.*, 4(1&2): 43 – 103.

(2) Fein, J. B., C. J. Daughney, N. Yee and T. A. Davis (1997). "A chemical equilibrium model for metal adsorption onto bacterial surfaces." *Geochim. Cosmochim. Acta* **61**(16): 3319 – 3328.

(3) Westall, J.C.; Jones, J.D.; Turner, G.D.; Zachara, J.M. Model for association of metal ions with heterogeneous environmental sorbents. 1. Complexation of Co(II) by Leonardite humic acid as a function of pH and $NaClO_4$ concentration. *Environ. Sci. Technol.* **1995**, 29, 951-959.

(4) Spadini, L.; Schindler, P.W.; Charlet, L.; Manceau, A.; Ragnarsdottir, K.V. Hydrous ferric oxide: evaluation of Cd–HFO surface complexation models combining Cd_K EXAFS data, potentiometric titration results, and surface site structures identified from mineralogical

knowledge. *J. Coll. Interf. Sci.* **2003**, 266, 1–18.

(5) Fein, J.B.; Boily, J-F.; Yee, N.; Gorman-Lewis, D.; Turner, B.F. Potentiometric titrations of *Bacillus subtilis* cells to low pH and comparison of modelling approaches. *Geochim. Cosmochim. Acta* **2005**, 69, 1123-1132.

(6) Ludwig, C. GRFIT: A program, for solving spection problems, evaluation of equilibrium constants, concentrations and their physical parameters. *University of Berne – Switzerland* **1992**.

(7) Jumpertz, E.A. Ueber die Elektronendichteverteilung in der Zinkblende. *Zeit. fuer Elektrochemie* **1955**, 59, 419-425.

(8) Reed, A.T.; Karipides, A. The crystal structure of S-Malatodiaquozinc(II) hydrate. *Acta Crystallogr.* **1976**, B32, 2085.

(9) Zabinsky, S.I.; Rehr, J.; Ankudinov, R.C.; Albers, R.; Eller, M.J. Multiple scattering calculations of X-ray absorption spectra. *Phys. Rev. B* **1995**, 52, 2995.

(10) Panfili, F.; Manceau, A.; Sarret, G.; Spadini, L.; Kirpichtchikova, T.; Bert, V.; Laboudigue, A.; Marcus, M.A.; Ahamdach, N.; Libert, M. The effect of phyto-stabilization on Zn speciation in a dredged contaminated sediment using scanning electron microscopy, X-ray fluorescence, EXAFS spectroscopy and principal components analysis. *Geochim. Cosmochim. Acta* **2005,** 69, 2265-2284.

(11) Sarret, G.; Manceau, A.; Spadini, L.; Roux, J.C.; Hazemann, J.L.; Soldo, Y.; Eybert-Berard, L.; Menthonnex, J.J. EXAFS determination of Pb, Zn complexing sites of *Penicillium chrysogenum* cell walls. *Environ. Sci. Technol.* **1998**, 32, 1648-1655.

(12) Beauchemin, S.; Hesterberg, D.; Nadeau, J.; McGeer, J.C. Speciation of hepatic Zn in trout exposed to elevated waterborne Zn using X-ray absorption spectroscopy. *Environ. Sci. Technol.* **2004**, 38, 1288-1295